Utilization of $As_{50}Se_{50}$ thin films in electron beam lithography

K. Palka[1,2*], M. Kurka[1], S. Slang[2], M. Vlcek[2]
[1] Department of General and Inorganic Chemistry ,Faculty of Chemical Technology, University of Pardubice, Studentska 95, 53210 Pardubice, Czech Republic
[2] Center of Materials and Nanotechnologies, Faculty of Chemical Technology, University of Pardubice, Studentska 95, 53210 Pardubice, Czech Republic
*karel.palka@upce.cz

Keywords: chalcogenide glasses, thin films, wet etching, electron beam lithography

Abstract
Chalcogenide glass of $As_{50}Se_{50}$ composition have been intensively studied for its interesting physical and chemical properties. Presented manuscript explores the applicability of $As_{50}Se_{50}$ thermally evaporated thin films in electron beam lithography exploiting wet etching in amine based solution. $As_{50}Se_{50}$ films proved to be highly sensitive negative resist. Decrease of the etching selectivity with increasing accelerating voltage and its increase with increasing exposure dose were observed. Height irregularities of prepared structures connected with the electron beam scattering and preferential etching of upper edges were observed and thoroughly studied. Comparison of photoinduced chemical resistance changes showed same trends as in case of electron beam induced changes – chemical resistance significantly increased with increasing exposure dosages.

Introduction

Chalcogenide glasses (ChG) are in the focus point of material science for many decades, predominantly for their remarkable optical properties such as wide transparency window in IR and high refractive index [1, 2]. Based on the composition, form and history of the sample, ChG are often photosensitive, which frequently leads to selective etching of the sample in alkaline solutions. Hence ChG can be used as inorganic photoresists for structuring of the undelaying material or to be structured themselves for desired application [3-5]. Multiple techniques such as photolithography, holography or embossing are frequently used [6-8]. Chalcogenide glasses are expected to achieve higher resolution in comparison with their organic counterparts due to smaller size of the structural units (molecular clusters) [4].
Electron beam lithography can be used for preparation of micro/nanostructures of highest resolution in chalcogenide thin films [9]. There are two mechanisms for preparation of surface structures in chalcogenide thin films by electron beam. First one is direct writing of structures by electron beam as was demonstrated in case of Ge-As-Se chalcogenide glass system [10, 11]. Second way for surface structuring is exposure of the latent image into the thin film followed by selective etching. The electron beam induces structural changes in the chalcogenide glass which results in changes in chemical resistance of exposed part of chalcogenide thin film leading to selective etching. The study of any structural changes induced by electron beam is generally challenging due to very small exposed area and thus small volume of the material.
Majority of the research on this topic have been done on the glasses of As-S system, particularly $As_{35}S_{65}$. It is assumed that electron beam induced changes in the glass properties are of similar nature as photoinduced changes [12] even though compositional changes on the surface are different [13]. This theory have been gradually confirmed by investigation of optical properties [14] and chemical resistance [9] of As-S thin films exposed to the electron beam. Obtained results showed analogy of photoinduced and electron beam induced changes such as significant increase of chemical resistance to amine based solutions, increase of the refractive index and decrease of the optical band gap (darkening).
ChG of $As_{50}Se_{50}$ composition have been intensively studied mostly for its optical properties [15-17], photoinduced changes in chemical resistance [18-20], crystallization kinetics [21, 22], Ag diffusion [23] or photoplastic effect [24].

Presented work describes the applicability of thermally evaporated $As_{50}Se_{50}$ thin films in electron beam lithography aiming for preparation of nanostructures. Due to the interesting optical properties finely structured $As_{50}Se_{50}$ thin films can be used directly in practical application or can be utilized as high resolution photoresist for transferring of the desired pattern into the underlying material. Influence of accelerating voltage and exposure dosage on etching selectivity in amine based solutions was investigated. Issues connected with electron beam exposure and consecutive wet etching are studied and discussed. Brief description of photoinduced changes is provided as well in order to compare their character.

Experimental

Source bulk $As_{50}Se_{50}$ chalcogenide glass was prepared by melt quenching method from high purity elements. Arsenic was purified from the arsenic oxide by sublimation right before loading of the ampule which was immediately evacuated and sealed. The synthesis was carried out in tube rocking furnace for 48 hours at 850 °C.

Thin films were prepared by vacuum thermal evaporation method using Tesla 858 device. Deposition rate ~1.5 nm/s and final thickness were measured in situ during the deposition by quartz crystal microbalance method (Inficon STM-2). Two sets of samples were prepared. The first one was deposited on silicate glass slides in 500 nm thickness. These samples were used for investigation of the structure, optical, chemical properties and their photoinduced changes. The second set of samples was deposited on silicate glass substrates coated with 20 nm thin film of carbon (Leica EM ACE200) used for grounding of the samples during electron beam lithography. Thickness of second set of samples was 100 nm. Electron beam exposures were performed at electron microscope Lyra 3 (Tescan).

Photosensitivity of $As_{50}Se_{50}$ thin films to VIS electromagnetic irradiation was studied using halogen lamp (120 mW/cm^2) with IR cut off filter in Ar atmosphere. Transmission spectra of as-prepared thin films and films exposed for various times to halogen lamp were measured using spectrometer UV-3600 (Shimadzu) and consequently evaluated by the procedure described in [25] providing optical parameters (optical band gap and spectral dependence of refractive index) of the thin films. Raman spectra were measured using IFS55/FRA106 (Bruker) spectrometer with Nd:YAG laser (1064 nm) as excitation source.

Procedure described in [26] was used for investigation of the etching kinetics of as-prepared and halogen lamp exposed thin films in 5% ethylenediamine solution in dimethyl sulfoxide using fiber spectrometer EPP2000 (StellarNet). Developing of the structure exposed by electron beam was carried out in 2% butylamine/dimethyl sulfoxide solution due to higher selectivity of butylamine in comparison with ethylenediamine as was demonstrated in [27].

Heights and depths of structures prepared by electron beam lithography were studied using AFM microscope Solver Next (NT-MDT) equipped with NSG10 tips (NT-MDT) in semicontact mode. Due to the dimensions of studied structures 10^1-10^2 nm, which are relatively close to the dimensions of the AFM tip itself, only heights of the structures were evaluated from the AFM scans. Proper measurement of the lateral dimensions of the structures would require deconvolution of the acquired scans, which would be very complicated considering number of AFM measurements discussed in this paper.

Results and discussion

Structural changes, and related changes in physical and chemical properties, induced by super band gap electromagnetic radiation and electron beam are expected to be similar [12]. In order to compare the impact of both kinds of irradiation on $As_{50}Se_{50}$ thin films properties, the photostructural changes induced by halogen lamp irradiation were studied alongside those induced by electron beam.

Raman spectra of as-prepared thin film, halogen lamp exposed thin film and source bulk glass are provided in Fig. 1. Structure of as-prepared thin film is highly disordered and consists mainly of As_4Se_3 cluster proved by the presence of the bands at 235 cm^{-1} in Raman spectra [28]. Additionally $AsSe_{3/2}$ polymer network is present as well (bands at 222 cm^{-1}) [29, 30]. Exposure to polychromatic VIS irradiation causes breakdown of the As_4Se_3 clusters and formation of $AsSe_{3/2}$ polymer network. Structure of fully exposed thin film is almost identical as the structure of source bulk material. Identical

photostructural changes have been observed in case of $As_{50}Se_{50}$ thin film exposures to monochromatic beams as well [16].

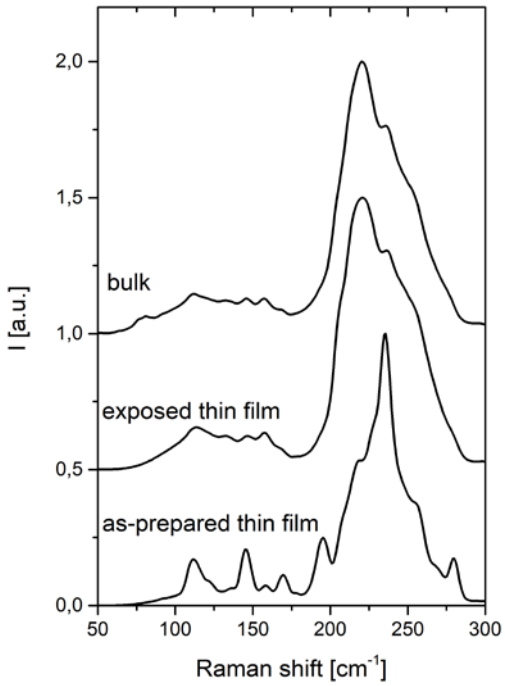

Fig.1 Raman spectra of as-deposited and exposed $As_{50}Se_{50}$ thin films and source bulk glass.

Significant photoinduced changes in the thin film structure substantially influence optical properties of the thin films (Fig. 2). Refractive index at 1550 nm increases from 2.65 to 2.80. Simultaneously values of optical band gap decrease from 1.89 to 1.71 eV. Photoinduced changes in optical properties are finished after ~8 min of exposure under given conditions, which suggests the structure to be fully transformed. Longer exposure times do not influence the values of observed optical properties.

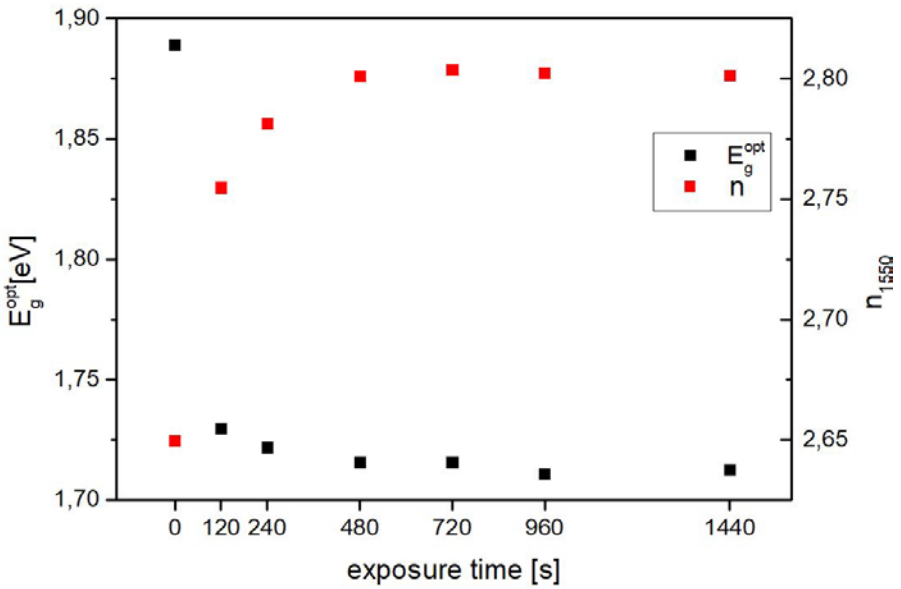

Fig. 2 Dependence of the refractive index ($\lambda = 1550$ nm) and optical band gap on the time of exposure to halogen lamp irradiation.

Chemical resistance of $As_{50}Se_{50}$ thin films is altered by the exposure to the halogen lamp radiation as well. Negative etching selectivity was observed (Fig. 3) - polymerization of the glass structure causes major increase in the glass chemical resistance to amine based developers, which is in good agreement

with [19]. The composition of used etching bath was 5% ethylenediamine solution in dimethyl sulfoxide. High value of etching selectivity ~150 (exposed areas etch off 150x slower in comparison with unexposed material) makes $As_{50}Se_{50}$ thin films very promising material for photolithography. Similarly to the photoinduced changes in optical properties, the chemical resistance doesn't change with prolonged exposure times after reaching the saturation at ~8 min.

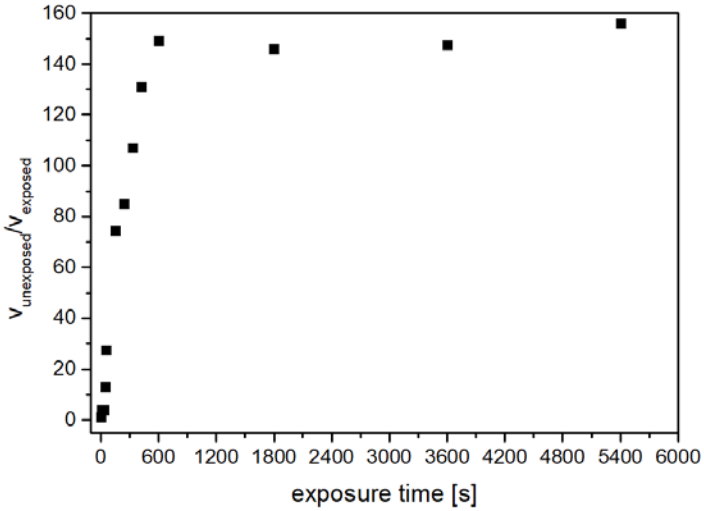

Fig. 3 Exposure time dependence of the etching selectivity of $As_{50}Se_{50}$ thermally evaporated thin films in 5% ethylenediamine in dimethyl sulfoxide solution.

There are two main parameters for electron beam exposure – the accelerating voltage determining the energy of the electrons and the exposure dosage. In order to determine the influence of both parameters the patterns of 5 μm squares with 5 μm gaps in between were written into the as-prepared $As_{50}Se_{50}$ thin films using accelerating voltages 5, 10, 15, 20, 25 and 30 kV and exposure dosages 30 – 6750 $\mu C.cm^{-2}$ for each used accelerating voltage. Exposed samples were etched in 2% butylamine in dimethyl sulfoxide solution for the time needed for dissolution of unexposed thin film. After the wet etching the exposed areas remained undissolved, which proves the negative etching selectivity of $As_{50}Se_{50}$ thermally evaporated thin films after electron beam exposure, same as in case of super band gap electromagnetic irradiation. Because the thickness of the original thin film (~100 nm) was constant for all studied structures, residual heights of the prepared structures provide an analogy with etching selectivity of the thin film dissolution (Fig. 3) – the greater is the residual height value the higher is the selectivity. Residual heights of prepared 5 μm squares in dependence on exposure dosages for all studied acceleration voltages are provided in Fig. 4 and hereinafter will be referred as saturation curves. Exposure dose dependences of the structure heights shows similar trend as in case of electromagnetic beam exposure – after reaching the limit value the height is no longer influenced by increased exposure dosage.

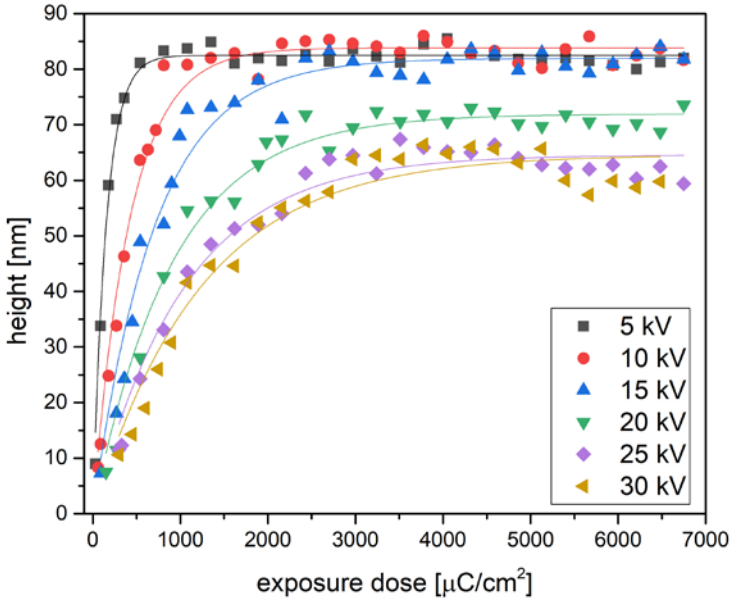

Fig. 4 Exposure dose dependence of the remaining heights of structures prepared using electron beam lithography in $As_{50}Se_{50}$ thin films.

Measured data for each used accelerating voltage were fitted by exponential stretch function widely used for describing the kinetics of the photoinduced changes in chalcogenides [31]:

$$h = A \cdot \left(1 - e^{\left(-\left(\frac{d}{\tau}\right)^{\beta}\right)}\right) \quad (1),$$

where h is the remaining height of the structure for the exposure dose d, parameter A is the limit height of the structure achievable by given accelerating voltage, τ is effective exposure dose and β the dispersion parameter. According to the simulations of electron penetration depths in Casino v2.4.8.1 program [32], the penetration depths of electrons for all used accelerating voltages are higher than the thickness of studied thin film, thus β parameter equals 1 [31]. The dependences of limit heights A and the effective exposure dose τ on used accelerating voltage are given in Fig. 5.

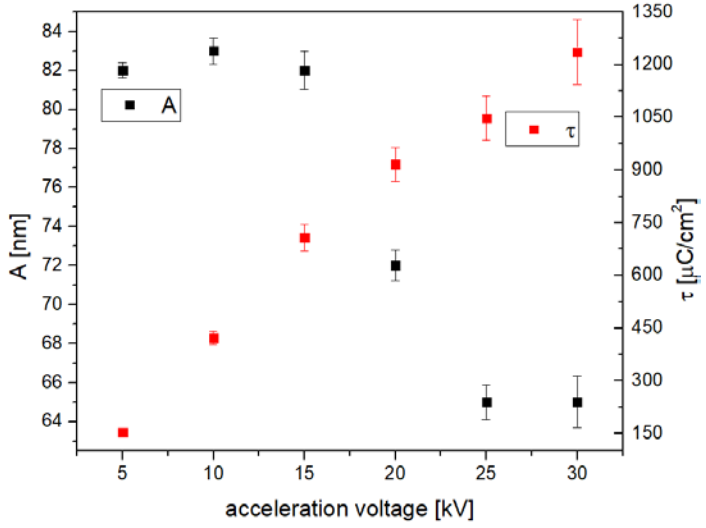

Fig. 5 Accelerating voltage dependences of limit height A (left) and effective exposure dose τ (right).

Accelerating voltage dependence of limit height A (Fig. 5) shows that exposures using acceleration voltages 5, 10 and 15 kV result in nearly identical limit height of the written structures. Further

increasing of the acceleration voltage causes significant decrease of the limit heights. Probable explanation for this phenomenon is the high energy of the electrons with accelerating voltages 20 – 30 kV, which does not cause full relaxation (polymerization) of the glass structure but due to the high energy of the electrons material is partially excited (fragmented) by the electron irradiation. Consequently, not fully polymerized glass structure exhibits only partially increased chemical resistance in comparison with fully polymerized structure, thus lower limit heights of prepared structures are observed.

Fig. 5 shows consistently increasing value of effective exposure dose τ with increasing accelerating voltage, thus with increasing accelerating voltage higher exposure doses are needed to achieve the limit high of prepared structures. Increasing accelerating voltage significantly increases the penetration depth of the electron beam. Consequently, smaller part of the electron's energy is transferred to the material, thus higher exposure dosages must be used.

Based on the saturation tests (Fig. 4) accelerating voltages 5 and 15 kV were selected for further experiments due to the highest achieved etching selectivity. Both induce similar changes in the thin films chemical resistance (Fig. 5 – parameter A) but penetration depths of the electrons are significantly different as is demonstrated in Fig. 6 (simulations were calculated in program Casino v2.4.8.1 [32]). Based on obtained saturation curves the basic exposure doses were determined as a dose needed for preparation of the structure with height corresponding to 99% of parameter *A*. The basic dose for 5 kV was 550 μC.cm^{-2} and 2200 μC.cm^{-2} for 15 kV.

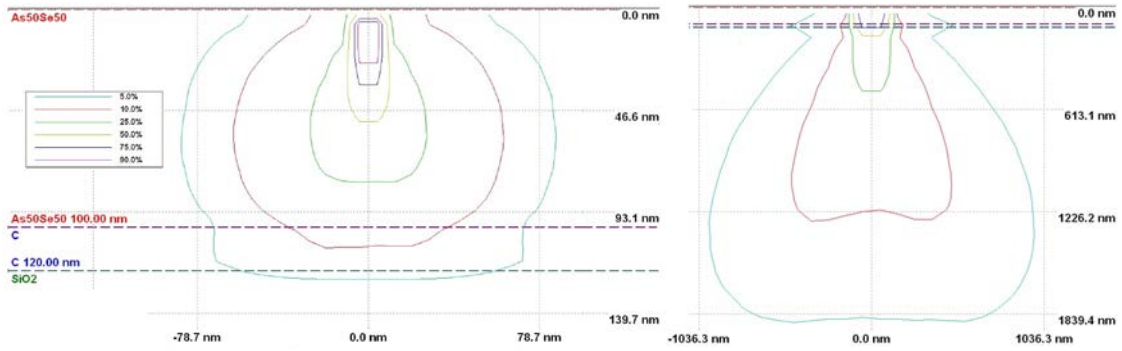

Fig. 6 Energy distribution profiles of electron beams at 5 kV (left) and 15 kV (right) in $As_{50}Se_{50}$ thin films simulated in Casino v2.4.8.1.

The influence of the lateral dimensions of micro/nanopatterns on the height of prepared structures was studied on linear periodic structures of widths 25, 50, 100, 200 and 400 nm in 1 μm period. Exposure dosages were chosen as 25, 50, 100, 150, 200 and 300% of basic dose for each accelerating voltage (138 - 1650 μC/cm^2 for 5 kV exposures and 550 - 6600 μC/cm^2 for 15 kV exposures).

Exposure dose dependences of the residual heights of structures prepared using 5kV accelerating voltage are presented in Fig. 7. Magenta line marks the theoretical height dependence on the exposure dosage calculated based on the parameters A and τ obtained from saturation curves (Fig. 4 and 5).

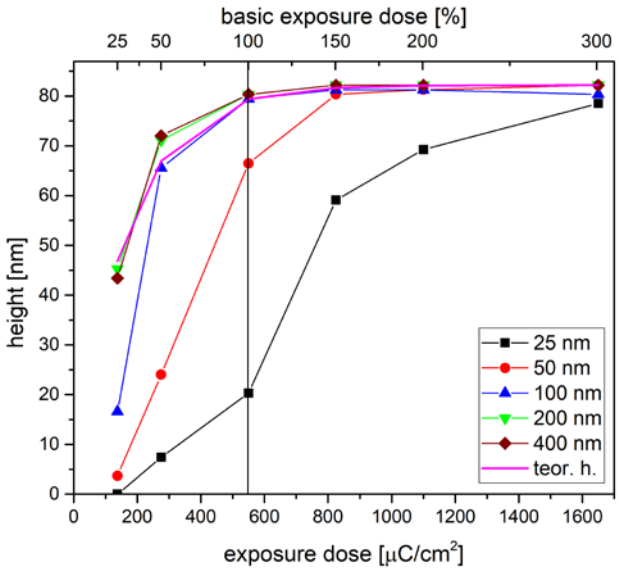

Fig. 7 Exposure dose dependences of the residual heights of linear structures (various widths) prepared using 5kV.

None of the structures prepared using 25 and 50% of the basic exposure dose does reach the limit height because of insufficient exposure dose thus the structure of the glass is not fully converted. Lines of 200 and 400 nm width follow the calculated theoretical height. Obtained data further give evidence that 100% of the basic exposure dosage (550 $\mu C.cm^{-2}$) is sufficient to reach the limit height of the structures ≥100 nm wide. On the other hand structures 25 and 50 nm wide reach only ~25% and ~83% respectively of the limit height. Exposure dose must be increased to 150% of the basic exposure dose in case of 50 nm wide structure and to 300% for 25 nm wide line in order to achieve the limit height of prepared structure given by the theoretical model (Fig. 7).

Possible explanation of this phenomenon could be found in preferential etching of the upper edges of written structures which are more intensively attacked by the etching solution (developer) due to the larger surface in comparison with flat top and side surfaces of the structure. Preferential etching consequently leads to the rounding of the structure. The height of the wide structures is not naturally influenced by this phenomenon (e.g. 5 μm squares used for saturation tests), but in case of very narrow structures eventual meeting of the rounded edges can ultimately result in decrease of the structure height (Fig. 8).

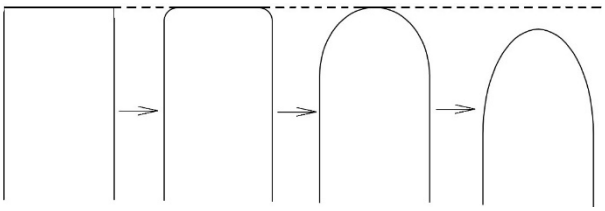

Fig. 8 Scheme of the preferential etching of the upper edges resulting in the height decrease of the structures.

Exceeding the basic exposure dose leads to the widening of the written structures due to significant scattering of the electron beam in the exposed sample (Fig. 6) and high sensitivity of the $As_{50}Se_{50}$ thin films to the electron beam (Fig. 4). Wider structures are less influenced by the height decrease by the edge rounding effect thus height of the structures after the wet etching increases with increasing exposure doses.

In order to study the influence of electron beam scattering on the quality of prepared structures, $As_{50}Se_{50}$ thin film was exposed by electron beam with various dosages using exposure pattern inverse

to previous experiment i.e. the sample was exposed in large area with unexposed lines of widths 25, 50, 100, 200 and 400 nm in 1 μm period left unexposed. Exposure dosages were chosen again 25, 50, 100, 150, 200 and 300% of basic exposure dose. Sample was consequently developed in the same manner revealing grooves in the unexposed areas of the sample. Depths of the grooves were measured using AFM and obtained data are provided in Fig. 9. Magenta line marks the theoretical depths dependence on the exposure dosage calculated based on the parameters A and τ obtained from saturation curves.

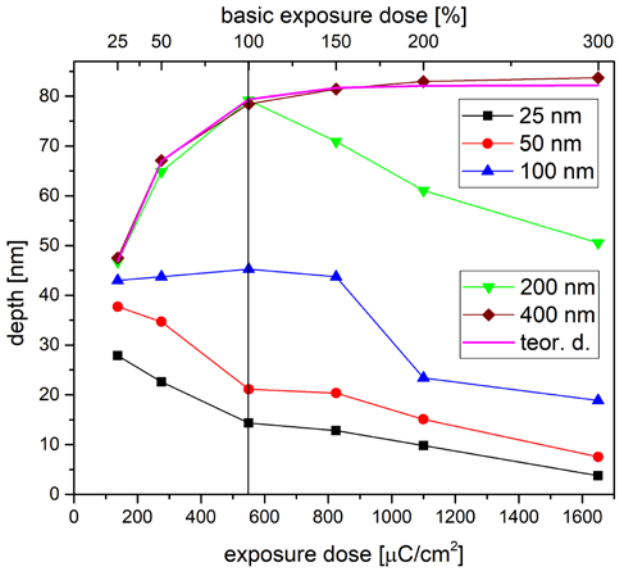

Fig. 9 Exposure dose dependences of the depth of grooves prepared using 5 kV accelerating voltage.

The widest 400 nm gaps follows the theoretical depth dose dependence thus no shallowing of the groove due to the scattering is observed. Similar behavior was observed in case of 200 nm wide gap for ≤100% of the basic exposure dosage. Higher exposure dosages resulted in decrease of the groove depth due the scattering of the electron beam. Narrow grooves 100, 50 and 25 nm show significant decrease in their depths in comparison with theoretical model even for the smallest exposure dosages. Increasing dosages further decreases the depth of the groove due to the scattering of the electron beam.

Same sets of structures (lines and grooves of various widths) as were studied using 5 kV accelerating voltage were exposed using 15 kV accelerating voltage to the $As_{50}Se_{50}$ thin films. Due to the higher energy of the electrons, the beam scattering is significantly higher (Fig. 6), which consequently manifested itself on obtained height and depths values of studied structures.

Dose dependence of the residual height of the lines exposed onto $As_{50}Se_{50}$ thin films using 15 kV accelerating voltage is presented in Fig. 10. Similar dose dependences were observed as in case of 5 kV exposures. Heights of 200 and 400 nm lines follow the theoretical values for exposure doses ≤100 % of the basic exposure doses. Lines 25-100 nm wide show significantly lower height in comparison with theoretical model, the height increases with increasing exposure dosages. Overexposed lines of width 50-400 nm show decreasing height with increasing exposure dosage and thickness of the exposed line. This phenomenon was not observed in case of 5 kV exposed lines and it could be explained by significantly higher scattering of the electron beam under 15 kV accelerating voltage (as proved by the theoretical simulation – Fig. 6). Scattering of the electron beam leads to partial exposure of the ChG in between of the exposed lines, which leads to local decrease of the etching rate a consequently results in remaining thin film of the glass in unexposed areas after the wet etching. Thus measured value of the lines height is decreasing not because of decreasing heights of the lines themselves but because of increasing thickness of the remaining thin film surrounding the prepared structures. Measured data are in good agreement with observed influence of beam scattering at 5 kV exposures.

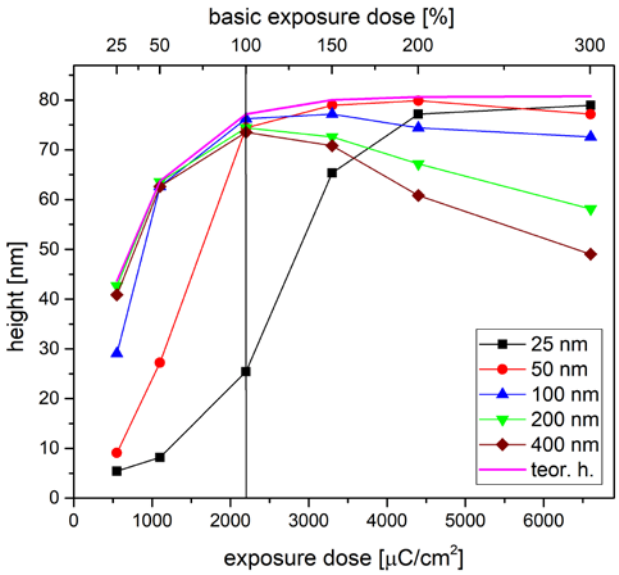

Fig. 10 Exposure dose dependences of the residual heights of structures prepared using 15 kV in $As_{50}Se_{50}$ thin films.

In order to verify the assumption about the influence of scattered electron beam, grooves of various widths were prepared in the same manner as in case of 5 kV exposures experiments. Values of measured depths of etched grooves together with theoretical dose dependence are provided in Fig. 11. Contrary to the 5 kV set of experiments all grooves prepared using 15 kV accelerating voltage are significantly shallower than theoretical depth while narrow grooves are influenced more in comparison with wide ones. Depth of the grooves further decreases with increasing exposure dosages.

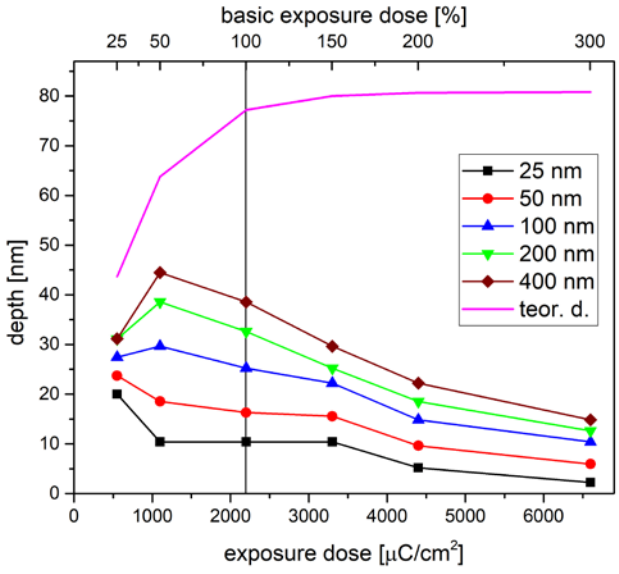

Fig. 11 Exposure dose dependences of the depth of grooves prepared using 15 kV accelerating voltage.

Electron beam lithography was used to prepare grating with 100 nm period in $As_{50}Se_{50}$ thin film (Fig. 12). Exposure was carried out at 5 kV accelerating voltage and applied dose was 550 $\mu C.cm^{-2}$ (basic dose). Obtained grating was of good quality despite observed issues such as edge rounding effect and

electron beam scattering, which successfully demonstrates applicability of the $As_{50}Se_{50}$ thin films as resists for electron beam lithography.

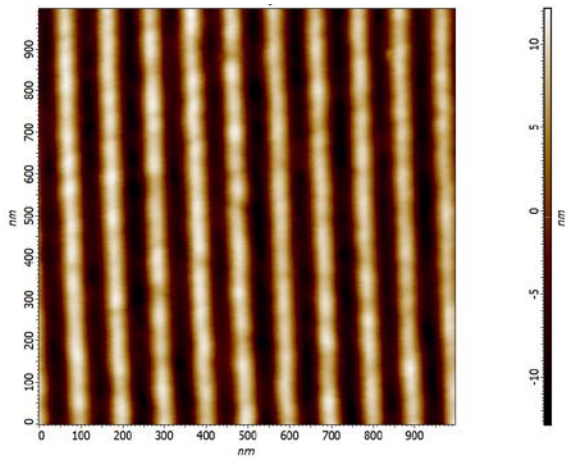

Fig. 12 Diffraction grating of 100 nm period prepared in $As_{50}Se_{50}$ thin film using electron beam litography.

Conclusion

Thermally evaporated $As_{50}Se_{50}$ thin chalcogenide films were proven as suitable material for electron beam lithography using selective wet etching in butylamine/dimethyl sulfoxide developer due to high sensitivity to electron beam and etching selectivity. Dependence of the etching selectivity on the used electron beam accelerating voltage showed decreasing etching selectivity with increasing accelerating voltage and contrary increasing selectivity with increasing exposure dose. Height irregularities of prepared micro/nanostructures were observed and explanations connected with preferential etching of the upper edges and electron scattering were suggested. Optimized exposure parameters were used for preparation of nanostructure – 100 nm period linear grating.

Photoinduced changes in chemical resistance showed similar trends as in case of electron beam induced changes – chemical resistance in etylenediamine/dimethyl sulfoxide solution increases with increasing exposure dosage. Additionally, photoinduced changes in optical properties and structure of $As_{50}Se_{50}$ thin films were investigated as well in order to provide deeper characteristic of studied material.

Acknowledgement

Authors appreciate financial support from the grants LM2015082 and "Modernization and upgrade of the CEMNAT" (No. CZ.02.1.01/0.0/0.0/16_013/0001829) from the Ministry of Education, Youth and Sports of the Czech Republic as well as European Regional Development Fund-Project “High sensitive sensors and low density materials based on polymeric nanocomposites – NANOMAT“ (No. CZ.02.1.01/0.0/0.0/17_048/0007376).

References

References

[1] K. Tanaka, K. Shimakawa, Amorphous Chalcogenide Semiconductors and Related Materials, Springer, New York 2011.

[2] J.-L. Adam, X. Zhang, Chalcogenide Glasses: Preparation, Properties and Applications, Woodhead Publishing, Cambridge 2014.

[3] H. Jain, A. Kovalskiy, Mir. Vlcek, Chalcogenide Glasses - Chalcogenide glass resists for lithography, Woodhead Publishing Limited (2014).

[4] H. Jain, Mir. Vlcek, J. Non-Cryst. Solids 354 (2008) 1401–1406.

[5] V. Lyubin, Phys. Status Solidi B, 246(8) (2009) 1758–1767.

[6] H. Xiong, Z. Wang, J. Micromech. Microeng. 29 (2019) 085002.

[7] J. Teteris, Curr. Opin. Solid St. M. 7 (2003) 127–134.

[8] H. Xiong, L. Wang, Z. Wang, J. Non-Cryst. Solids 521(2019) 119542.

[9] A. Kovalskiy, J. Cech, Mir. Vlcek, C.M. Waits, M. Dubey, W.R. Heffner and H. Jain, MEMS MOEMS 8(4) (2009) 043012.

[10] V. Bilanych, V. Komanicky, M. Kozejova, A. Feher, A. Kovalcikova, F. Lofaj, V. Kuzma, V. Rizak, Thin Solid Films 616 (2016) 86–94.

[11] V. Kuzma, V. Bilanych, M. Kozejova, D. Hlozna, A. Feher, V. Rizak, V. Komanicky, J. Non-Cryst. Solids 456(2017 7-11.

[12] A. Kovalskiy, Mir. Vlcek, H. Jain, A. Fiserova, C.M. Waits, M. Dubey, J. Non-Cryst. Solids 352 (2006) 589–594.

[13] A. Kovalskiy, J.R. Neilson, A.C. Miller, F.C. Miller, Mir. Vlcek, H. Jain, Thin Solid Films 516 (2008) 7511-7518.

[14] P. Janicek, S. Funke, P.H. Thiesen, S. Slang, K. Palka, J. Mistrik, M. Grinco, Mir. Vlcek, Thin Solid Films 660 (2018) 759–765.

[15]] P. Nemec, J. Jedelsky, M. Frumar, M. Stabl, Z. Cernosek, Thin Solid Films 484 (2005) 140– 145.

[16] K. Palka, Mir. Vlcek, J. Mistrik, J. Optoelectron. Adv. M. 13 (11-12) (2011) 1510-1513.

[17] E. Flaxer, M. Klebanov, D. Abrahamoff, S. Noah, V. Lyubin, Opt. Mater. 31 (2009) 688–690.

[18] A. Feigel, Z. Kotler, and B. Sfez, A. Arsh, M. Klebanov, and V. Lyubin, Appl. Phys. Lett. 77 (20) (2000) 3221-3223.

[19] K. Palka, Mir. Vlcek, A. Kovalskiy Phys. Procedia 44 (2013) 114 – 119.

[20] V. Lyubin, M. Klebanov, I. Bar, S. Rosenwaks, N. P. Eisenberg, M. Manevich, J. Vac. Sci. Technol. B 15 (1997) 823-827.

[21] M. Mohamed, A. Y. Abdel-Latief, M. A. Abdel-Rahim, N. M. A. Hadia, E. R. Shaaban, M. N. Abd-el Salam, Applied Physics A 124 (8)(2018) 562.

[22] A.V Kolobov, P. Fons, J. Tominaga, Phys. Status Solidi B, 251 (7) (2014) 1297–1308.

[23] M. Kalyva, A. Siokou, S.N. Yannopoulos, T. Wagner, J. Orava, M. Frumar, J. Non-Cryst. Solids, 355 (2009) 1844–1848.

[24] M. L. Trunov, S. N. Dub, R. S. Shmegera, J. Optoelectron. Adv. M. 7 (2) (2005) 619 – 624.

[25] K. Palka, S. Slang , J. Buzek, Mir. Vlcek, J. Non-Cryst. Solids, 447 (2016) 104-109.

[26] L. Loghina, K. Palka, J. Buzek, S. Slang, Mir. Vlcek, J. Non-Cryst. Solids 430 (2015) 21–24.

[27] K. Palka, J. Jancalek, S. Slang, M. Grinco, Mir. Vlcek, J. Non-Cryst. Solids, 508 (2019) 7-14.

[28] P. Nemec, M. Frumar, Thin Solid Films, 516 (2008) 8377-8380.

[29] V. Kovanda, Mir. Vlcek, H. Jain, J. Non-Cryst. Solids 326 (2003) 88-92.

[30] M.S. Iovu, E.I. Kamitsos, C.P.E. Varsamis, P. Boolchand, M. Popescu, J. Optoelectron. Adv. M. 7 (3) (2005) 1217-1221.

[31] K. Shimakawa, N. Nakagawa, T. Itoh, Appl. Phys. Lett. 95 (2009) 051908.

[32] D. Drouin, A.R. Couture, D. Joly, X. Tastet, V. Aimez, R. Gauvin, Scanning 29 (2007) 92-101.